# Fabrication of an asymmetric Bragg coupler-based polymeric filter with a single-grating waveguide

**Wei-Ching Chuang,[1] Yu-Tai Huang,[1] Hui-Chi Lin,[1] and An-Chen Lee [2]**

[1]*Department of Electro-Optical Engineering, National Formosa University, Huwei, Yunlin, Taiwan*
[2]*Department of Mechanical Engineering, National Chiao Tung University, Hsinchu, Taiwan*
*eocwc@nfu.edu.tw*

**Abstract:** In this work, a first report on fabricating an asymmetric Bragg coupler-based filter on polymeric waveguides without input-waveguide grating was revealed. The fabrication process we developed was using holographic interference techniques, capillary effect, soft lithography, and micro molding process. The transmission dip of about –9.2 dB and the 3 dB transmission bandwidth of about 0.125 nm were obtained from a filter.



**OCIS codes:** (090.2880) Holographic interferometry; (050.2770) Gratings; (130.7408) Wavelength filtering devices; (160.5470) Polymers; (130.5460) Polymer waveguides; (230.7380) Waveguides, channeled.

## References and links

1. D. Mechin, P. Grosso, and D. Bose, "Add-drop multiplexer with UV-written Bragg gratings and directional coupler in $SiO_2$-Si integrated waveguides," J. Lightwave Technol. **19**(9), 1282–1286 (2001).
2. J. M. Simmons, "On determining the optimal optical reach for a long-haul network," J. Lightwave Technol. **23**(3), 1039–1048 (2005).
3. P. G. Arbués, G. M. Machuca, and A. Tzanakaki, "Comparative study of existing OADM and OXC architectures and technologies from the failure behavior perspective," J. Opt. Netw. **6**(2), 123–133 (2007).
4. T. Barwicz, M. A. Popović, P. T. Rakich, M. R. Watts, H. A. Haus, E. P. Ippen, and H. I. Smith, "Microring-resonator-based add-drop filters in SiN: fabrication and analysis," Opt. Express **12**(7), 1437–1442 (2004).
5. S. Xiao, M. H. Khan, H. Shen, and M. Qi, "A highly compact third-order silicon microring add-drop filter with a very large free spectral range, a flat passband and a low delay dispersion," Opt. Express **15**(22), 14765–14771 (2007).
6. L. Eldada, Shing Yin, C. Poga, C. Glass, R. Blomquist, and R. A. Nonvood, "Integrated multichannel OADM's using polymer Bragg grating MZI's," IEEE Photon. Technol. Lett. **10**(10), 1416–1418 (1998).
7. S. Ahn, and S. Shin, "Post-fabrication tuning of a polymeric grating-assisted co-directional coupler filter by photobleaching," Opt. Commun. **194**(4-6), 309–312 (2001).
8. T. Erdogan, "Optical add-drop multiplexer based on an asymmetric Bragg coupler," Opt. Commun. **157**(1-6), 249–264 (1998).
9. M. Oh, H. Lee, M. Lee, J. Ahn, S. G. Han, and H. Kim, "Tunable wavelength filters with Bragg gratings in polymer waveguides," Appl. Phys. Lett. **73**(18), 2543–2545 (1998).
10. L. Zhu, Y. Huang, W. M. J. Green, and A. Yariv, "Polymeric multi-channel bandpass filters in phase-shifted Bragg waveguide gratings by direct electron beam writing," Opt. Express **12**(25), 6372–6376 (2004).
11. W. C. Chuang, C. K. Chao, and C. T. Ho, "Fabrication of high-resolution periodical structure on polymer waveguides using a replication process," Opt. Express **15**(14), 8649–8659 (2007), http://www.opticsinfobase.org/abstract.cfm?URI=oe-15-14-8649.
12. Q. Xu, D. Fattal, and R. G. Beausoleil, "Silicon microring resonators with 1.5-microm radius," Opt. Express **16**(6), 4309–4315 (2008).
13. W. C. Chuang, A. C. Lee, C. K. Chao, and C. T. Ho, "Fabrication of optical filters based on polymer asymmetric Bragg couplers," Opt. Express **17**(20), 18003–18013 (2009).
14. J. Scheuer, and A. Yariv, "Fabrication and characterization of low-loss polymeric waveguides and micro-ring," J. Eur. Opt. Soc. Rapid Publ. **1**, 06007 (2006).
15. D.-Y. Choi, S. Madden, A. Rode, R. Wang, B. Luther-Davies, N. J. Baker, and B. J. Eggleton, "Integrated shadow mask for sampled Bragg gratings in chalcogenide ($As_{(2)}S_{(3)}$) planar waveguides," Opt. Express **15**(12), 7708–7712 (2007).
16. J.-W. Kang, M.-J. Kim, J.-P. Kim, S.-J. Yoo, J.-S. Lee, D. Y. Kim, and J.-J. Kim, "Polymeric wavelength filters fabricated using holographic surface relief gratings on azobenzene-containing polymer films," Appl. Phys. Lett. **82**(22), 3823–3825 (2003).

#143147 - $15.00 USD Received 23 Feb 2011; revised 28 Apr 2011; accepted 1 May 2011; published 18 May 2011

17. R. Horvath, H. C. Pedersen, N. Skivesen, C. Svanberg, and N. B. Larsen, "Fabrication of reverse symmetry polymer waveguide sensor chips on nanoporous substrates using dip-floating," J. Micromech. Microeng. **15**(6), 1260–1264 (2005).
18. T. L. Lowder, J. D. Gordon, S. M. Schultz, and R. H. Selfridge, "Volatile organic compound sensing using a surface-relief D-shaped fiber Bragg grating and a polydimethylsiloxane layer," Opt. Lett. **32**(17), 2523–2525 (2007).
19. J. J. Wang, L. Chen, S. Kwan, F. Liu, and X. Deng, "Resonant grating filters as refractive index sensors for chemical and biological detections," J. Vac. Sci. Technol. B **23**(6), 3006–3010 (2005).
20. L. Eldada, R. Blomquist, M. Maxfield, D. Pant, G. Boudoughian, C. Poga, and R. A. Norwood, "Thermooptic planar polymer Bragg grating OADM's with broad tuning range," IEEE Photon. Technol. Lett. **11**(4), 448–450 (1999).
21. J. H. Lee, M. Y. Park, C. Y. Kim, S. H. Cho, W. Lee, G. Jeong, and B. W. Kim, "Tunable External Cavity Laser Based on Polymer Waveguide Platform for WDM Access Network," IEEE Photon. Technol. Lett. **17**(9), 1956–1958 (2005).
22. Y. Zhu, E. Simova, P. Berini, and C. P. Grover, "A comparison of wavelength dependent polarization dependent loss measurements in fiber gratings," IEEE Trans. Instrum. Meas. **49**(6), 1231–1239 (2000).
23. R. G. Hunsperger, *Integrated Optics: Theory and Technology* (Springer, 2009).

## 1. Introduction

Optical add/drop multiplexer (OADM) devices, enabling the flexible insertion (add) or extraction (drop) of a specific wavelength in optical fiber communications, have been indispensable components for wavelength division multiplexing (WDM)-based networks, accommodating large bandwidths for the global spread multimedia communications. These components not only allow the extraction of a wavelength from a transmission loop and the addition of the same wavelength to the network [1,2], but also, monitor the signals in transparent networks to identify and locate the possible failures [3]. Numerous different architectures of OADMs, based on different optical devices have been revealed, such as array waveguide gratings, fiber-based, and integrated optics-based devices. Among them, the integrated optics-based devices attract more attention for their compactness, mechanical stability and suitability for mass-production, as well as the inclusion of several functions on a single chip. These include micro-ring resonators [4,5], Mach-Zehnder interferometer (MZI) based add/drop filters [6], grating-assisted co-directional couplers [7], asymmetric Bragg coupler (ABC) based filters [8], and Bragg reflector channel waveguide filters [9–11]. Micro-ring resonators have been the promising devices and used as passive and active components due to their unique properties. However, they generally suffer from either a narrow free spectral range (FSR), or an expensive fabrication equipment [12], that restrict its application range in WDM networks. The merits and drawbacks of the other devices have been depicted in our previous paper [13]. The performance and characteristics of ABC-based filters, based on a single grating in one arm of a non-resonant coupler and operated in a contra-directional mode, have been examined in detail [8].

In integrated optics or guided wave optics, high quality and inexpensive materials are required for highly-integrated photonic processors. Polymeric materials possess unique optical and mechanical properties [14] such as relatively low refractive index resulting in lower surface-roughness scattering, easily manipulating by conventional or unconventional fabrication technologies, providing excellent platform for integrating numerous materials with different functions, and high flexibility for being bent and attached to non-planar surface. Additionally, they are cost-effective and reliable for mass-production. Polymer surface-relief Bragg grating, which provides a narrow bandwidth, low crosstalk, and flat-top pass band, has become an essential component for various applications in optical communications and optical sensing [15]. For example, J. Kang et al [16] demonstrated a narrow band filter of 0.2 nm bandwidth using polymer surface-relief Bragg grating on an integrated optical waveguide. R. Horvath et al [17] fabricated a cost-effective polymer waveguide sensor chip using polymer surface-relief Bragg grating integrated on polymer film as a light coupler. Other application of tunable laser and filters were demonstrated in Ref [18–21].

In the past, we demonstrated a process to rapidly produce submicron range gratings on a polymeric waveguide for optical filters [11]. A high aspect ratio and vertical sidewalls are obtained, and consistent reproduction of the grating on a UV polymer has been achieved.

#143147 - $15.00 USD Received 23 Feb 2011; revised 28 Apr 2011; accepted 1 May 2011; published 18 May 2011

Recently, we combined the holographic interferometry, soft lithography, and a simple replication processes for fabricating a polymeric ABC filter [13]. The method includes the following procedures. The grating structure on a polymer was first fabricated using holographic interferometry and the micro-molding processes. An ABC filter was produced by a two-step molding process where the master mold was first formed on negative tone photoresist and subsequently transferred to a PDMS mold; following this step, the PDMS silicon rubber mold was used as a stamp to transfer the pattern of polymeric ABC filter onto a UV cure epoxy. Narrow bandwidths and deep transmission dips were obtained. However, the device has a disadvantage that the gratings were engraved concurrently on the bottoms of a pair of dissimilar waveguides, embedded into a planar substrate, and therefore an undesired reflection wavelength, denoted by self-reflection Bragg wavelength, caused by the grating of input waveguide was occurred in the input end. In order to overcome the above drawback, we develop a process, incorporating the above technologies with capillary effect and microscopy technologies to fabricate an ABC filter without any self-reflections.

Polymeric ABC filters were constructed using the planar channel waveguide configuration. A pair of parallel channel waveguides with different widths was proximally embedded into a planar substrate. These two waveguides are asynchronous because the effective indices of the two waveguides are quite different. In spite of the large index mismatch between the two waveguides, an efficient power coupling was achieved using the Bragg grating, engraved on the bottom of the either/both waveguides. Due to the close proximity of the two waveguides, engraving the grating on the bottom of the either waveguide is much more difficult than that of the both ones. However, if the gratings are engraved on the bottoms of both waveguides, the maximum self- and cross-reflection power coupling simultaneously occurred in the input and drop ports, respectively. The self-reflection light results in broadening the transmission spectrum of the filters because of spectral overlapping with the cross-reflection one. In the previous work, we made the two decoupled waveguides quite dissimilar to avoid the spectrum overlapping. In this paper, we develop a process, comprising of capillary effect and microscopy technologies, to eliminate the self-reflection light by removing the grating of the input waveguide; the schematic diagram of an ABC-based polymeric filter is depicted in Fig. 1. It is noted that there is no grating on the input waveguide. To our best knowledge, it is the first report for ABC structures with a single-grating waveguide on polymeric materials.

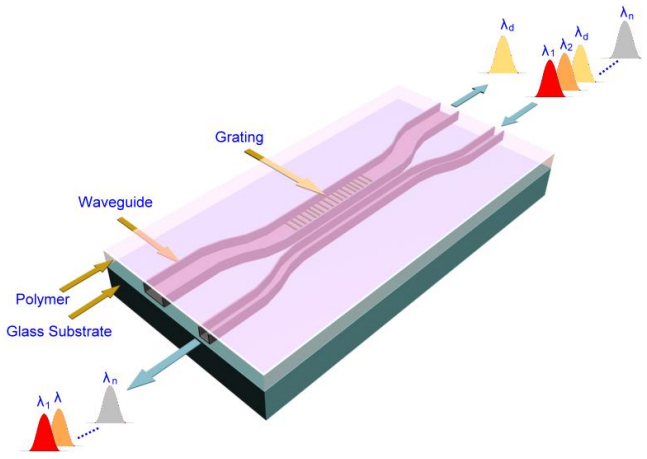


Fig. 1. Schematic of an asymmetric Bragg coupler (ABC)-based polymeric filter without input-waveguide grating.

#143147 - $15.00 USD Received 23 Feb 2011; revised 28 Apr 2011; accepted 1 May 2011; published 18 May 2011

## 2. Asymmetric waveguide coupler fabrication

A three-step process for rapid prototyping of an intaglioed asymmetric waveguide coupler structure on a polymer substrate was carried out first. A 700-μm thick glass substrate was first cut into a 5 cm × 1 cm rectangle. After substrate cleaning, the UV polymer layer (OG 146, Epoxy Technology Inc., USA) was deposited on the glass; it was coated with 6.0 μm thick negative photoresist (SU8) spun on at 1000 rpm for 17 seconds. An asymmetric waveguide coupler pattern was exposed on the negative photoresist film through polyethylene terephthalate (PET)-based mask using a UV mask aligner (AB-manufacturing, CA) for 9 seconds; this was followed by development in a SU-8 developer (MicroChem Corp., MA) for 45 seconds to obtain a negative waveguide coupler pattern (Fig. 2(a)-(c)). This produced a master that was subsequently used to produce a polydimethylsiloxane (PDMS) mold. This silicone rubber mold was then used as a stamp to transfer the intaglioed waveguide pattern onto a UV cure polymer (Ormo-comp, micro resist technology GmbH, Berlin). The optical microscope (OM) image shows the end-face of the cross-section of the mold (Fig. 3).

In order to eliminate the self-reflection from the input terminal, the grating of the waveguide mold was made on either side (drop terminal) of the asymmetric waveguides. A precured h-PDMS, being with low viscosity, was injected into the narrower waveguide groove with capillary effect using a dripping needle, assembled on a micro-positioning stage with resolution of 0.1 μm, under the inspection of a long-working-distance microscope (ZAK microscopes, Taiwan). The focal length of the objective is 13 mm. After baking at 90 °C for 1 hour, the h-PDMS was cured to act as a protection layer to prevent the forming of grating pattern on the narrower waveguide. After spin-coating a positive photoresist (Ultra 123, MicroChem Corp., MA) on the polymer mold, a grating pattern was holographically exposed using a two beam interference pattern on the positive photoresist film; this was followed by development in a Ultra 123 developer (Fig. 2(d)-(g)). In order to peel off the protection layer, which is lapsed into the groove of the waveguide mold, a PDMS film was spun on the waveguide mold; followed by 90 °C baking for 1 hour, and then, peeled off the PDMS film. At this stage, the first waveguide mold was accomplished (Fig. 2(h)-(j)). The OM image (Fig. 4) shows the positive photoresist filled into the groove of the wider waveguide after spin coating.

#143147 - $15.00 USD Received 23 Feb 2011; revised 28 Apr 2011; accepted 1 May 2011; published 18 May 2011

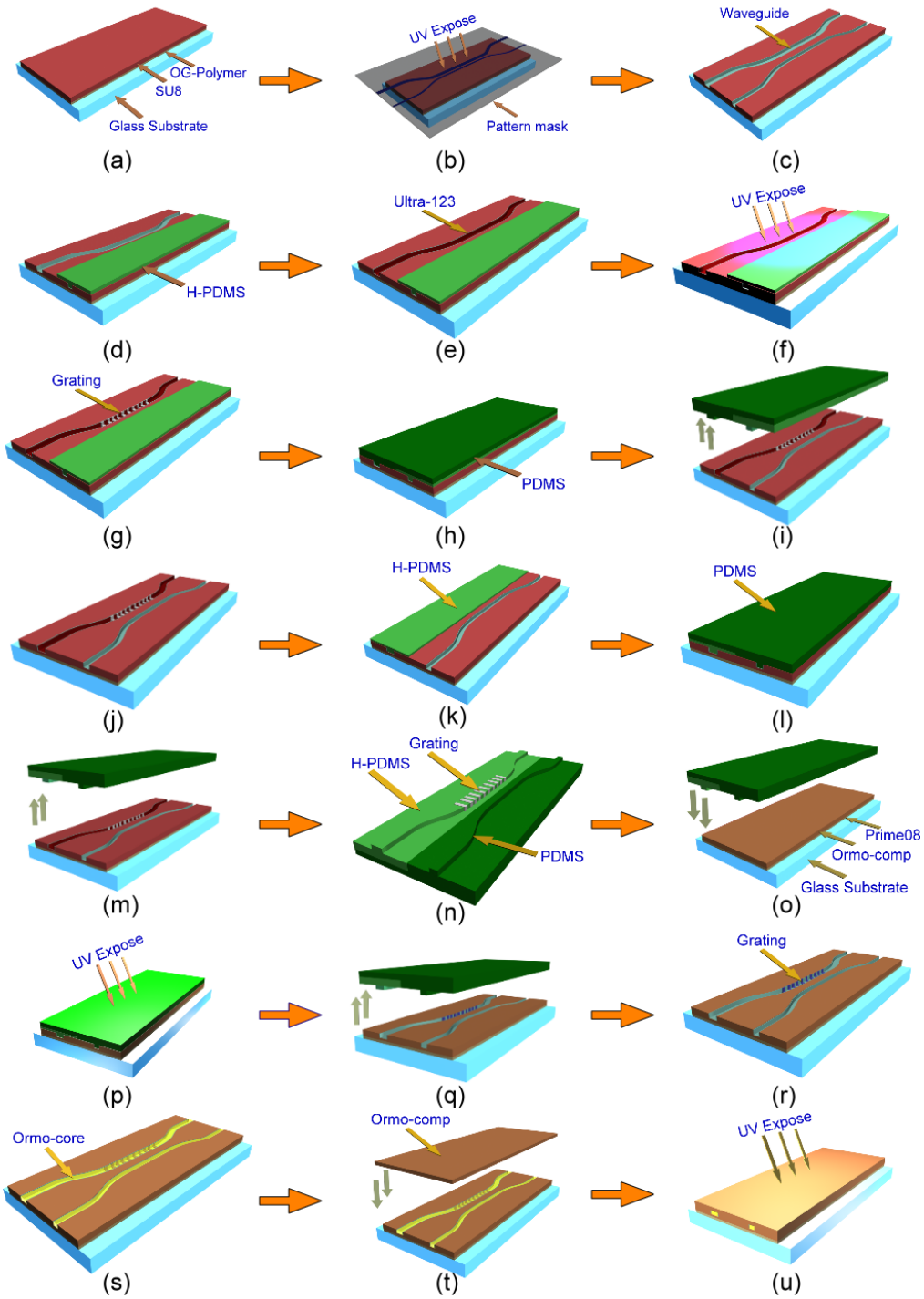


Fig. 2. Fabrication process of buried grating in polymeric waveguide filter structure:(a) A negative photoresist and UV polymer are deposited on the glass (b) The photoresist is exposed to the UV light through a photo mask (c) The asymmetric waveguide coupler mold (d) H-PDMS is injected into a waveguide of the photoresist mold (e) The positive photoresist is deposited on the mold (f) The grating is holographically exposed on the positive photoresist of the mold (g) The grating is patterned on an alternative waveguide of the mold (h) The PDMS is

#143147 - $15.00 USD Received 23 Feb 2011; revised 28 Apr 2011; accepted 1 May 2011; published 18 May 2011

spun on the mold (i) The PDMS adhered with H-PDMS is removed to form a master mold (j) The master mold (k) The H-PDMS is injected into the grating-engraved waveguide (l) The PDMS is spun on the master mold to form a stamp (m) The PDMS adhered with H-PDMS is removed to obtain a stamp (n) The stamp mold (o) An ABC pattern is transferred from PDMS stamp to an Ormo-comp polymer (p) The Ormo-comp polymer is exposed to a wide band UV light (q) The PDMS stamp is removed (r) A hardened Ormo-comp polymer forms a cladding layer of the ABC filter (s) An Ormo-core polymer is injected into the channel to form the waveguide core (t) An Ormo-comp polymer is deposited (u) The Ormo-comp layer is cured by exposing the UV light to form the final filter.

The patterned photoresist was used as a mother mold to transfer the pattern onto a h-PDMS film using typical micro-molding techniques (e.g. stamping). Instead of PDMS, resulting in a sticking effect in a high-aspect-ratio grating fabrication, a precured h-PDMS was injected into the grating-engraved waveguide groove using the capillary effect, the techniques mentioned above.After baking at 90 °C for 1 hour, the h-PDMS was cured; this was followed by spinning a PDMS film on the mold, and then, after baking at 90 °C for 1 hour, a stamp mold was obtained by peeling off the PDMS film from the master mold (Fig. 2(k)-(n)). An SEM image of the stamp mold was taken after the PDMS mold was fabricated (Fig. 5), showing the intact grating on a waveguide of the coupler mold. The grating period and depth are about 500 nm and 400-450 nm, respectively. These two quantities were measured using an atomic force microscope (AFM). The waveguides with a single grating pattern was transferred onto a UV polymer (Ormo-comp, refractive index = 1.505@1550 nm, micro resist technology, GmbH, Berlin) from the PDMS mold using UV replication process described by our previous report.

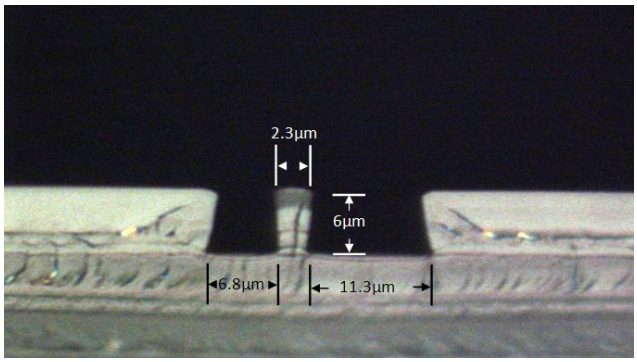


Fig. 3. Optical-microscope photograph of an asymmetric waveguide coupler pattern on SU8 photoresist; the cross-sectional dimensions are 6.8 μm × 6 μm and 11.3 μm × 6 μm and the gap is about 2.3 μm.

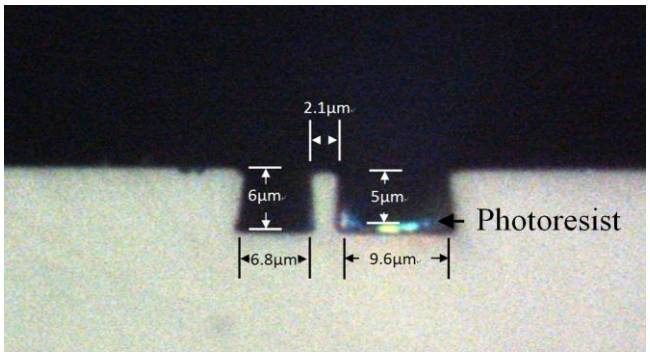


Fig. 4. Optical-microscope photograph of an asymmetric Bragg coupler mold; the positive photoresist filled into the wider waveguide groove; the final cross-sectional dimensions are 6.8 μm × 6 μm and 9.6 μm × 5 μm, and the gap is about 2.1 μm.

#143147 - $15.00 USD Received 23 Feb 2011; revised 28 Apr 2011; accepted 1 May 2011; published 18 May 2011

In order to enhance the adherence between the UV polymer (Ormo-comp) and the glass substrate, an adhesion promoter, prime 08, was deposited on a thin Pyrex glass slide. A spacer with a thickness of 30 μm was placed between the mold and the prime 08 film, deposited on the thin Pyrex glass slide. After injecting the precured UV polymer (Ormo-comp), the epoxy was then cured under a broadband UV light operating in a wavelength range of 300-400 nm. After the polymer was completely cured, it was easily peeled off from the mold (Fig. 2 (o)-(r)). The SEM image (Fig. 6) shows that the replication on UV polymer is good, and matches the negative photoresist mold dimension well. After separated from the PDMS mold, a hardened epoxy with single grating is formed as the cladding layer of the polymer ABC waveguide filter. For sample1 (Fig. 6), the cross-sectional dimensions of waveguide grooves are 6 μm × 6.9 μm (without grating) and 5 μm × 9.7 μm (with grating); the gap is about 2.4 μm; the coupling length is about 15 mm, and the total length is about 5 cm.

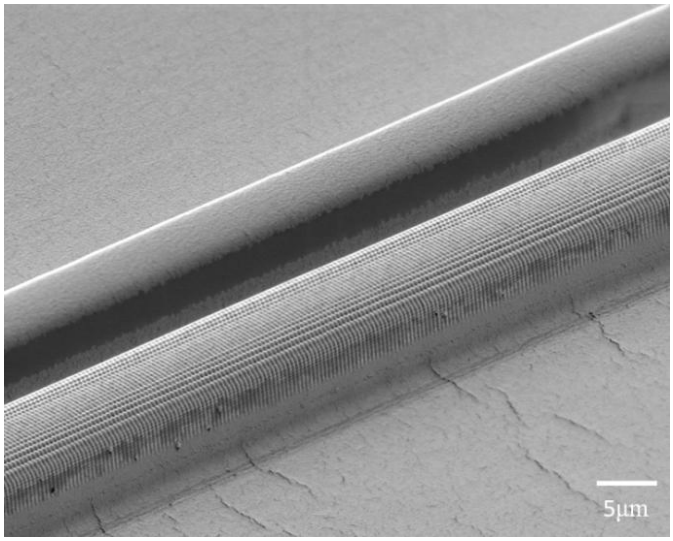


Fig. 5. SEM micrograph of the PDMS-hPDMS waveguide with grating; the SEM was titled about 30° (the grating period is 500 nm and the depth is about 450 nm).

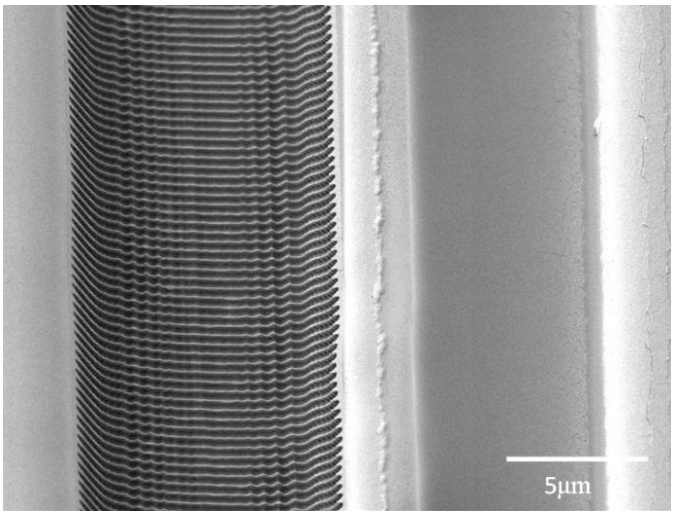


Fig. 6. SEM micrograph of the UV epoxy groove showing the intact grating pattern inside the groove (the dimensions are 6.8 μm × 6 μm and 9.6 μm × 5 μm, the gap is about 2.4 μm, the grating length is about 15 mm, and the grating depth is about 450 nm.

#143147 - $15.00 USD Received 23 Feb 2011; revised 28 Apr 2011; accepted 1 May 2011; published 18 May 2011

To form the waveguide core, another UV epoxy (Ormo-core, refractive index = 1.539 @1550 nm) was injected into the grooves. Instead of using the spin-coating technique, which could cause a thick unguided layer outside the core region, resulting in some coupling loss during the input of the optical fiber to the filter, another simple method was proposed. A pre-cured UV epoxy was dripped into the grooves of the channel waveguides from an optical fiber, sharpened by using of a fusion splicing machine and suspended from a micro-positioning probing stage, under the inspection of a long-working-distance optical microscope. After the precured UV epoxy was fully filled into the grooves, a PDMS layer was spun on a slide glass and placed over the top of the waveguide grooves to extrude the otiose epoxy outside the core region under a proper pressure; then, the UV epoxy was cured by exposure under the broadband UV light. After the cover glass was removed, the PDMS layer was peeled off from the sample (Fig. 2(s)).

In order to prevent optical loss due to either surface scattering losses or the outright absence of a guided mode for the asymmetric waveguide structure, the upper cladding layer was used. The same UV epoxy (Ormo-comp) was deposited using the procedure described in the previous section. A spacer with a thickness of 30 μm was placed between the sample and a thin Pyrex glass slide. After injecting the pre-cured UV polymer (Ormo-comp) into the opening between the sample and the glass slide, UV light was used to crosslink the polymer. The sample was diced and the end-faces were polished; the final polymeric ABC filter was 4 cm in length, 1 cm in width and approximately 60 μm in thickness (Fig. 2(t)-(u)). Figure 7 shows the cross-sectional view of the two asymmetric waveguides in the output end. Obviously, there is no unguided layer outside the core region.

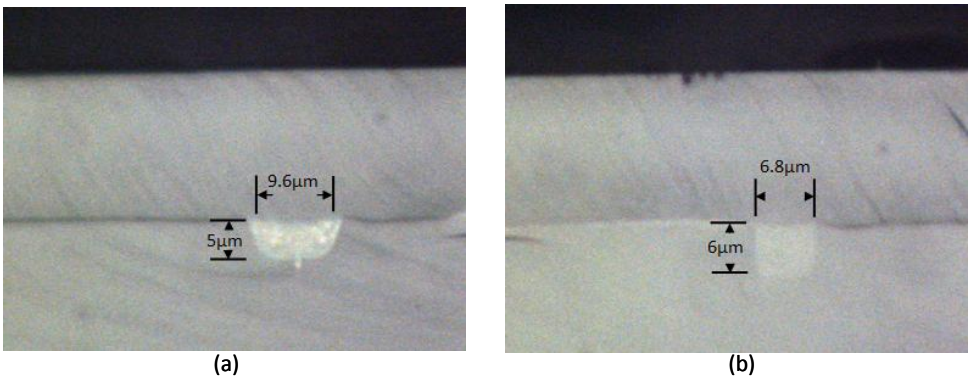


Fig. 7. Optical-micrograph of the output end of an ABC-based filter (a) the wider waveguide (cross-sectional dimension is 5 μm × 9.6 μm), and (b) the narrower waveguide (cross-sectional dimension is 6 μm × 6.8 μm). It shows that there is no unguided layer outside the core region.

## 3. Simulation

The essential waveguide properties, including the mode patterns and effective refractive indexes, were investigated using the finite different time domain beam propagation method (FDTD-BPM); the device transmission characteristics, including the minimum transmission and the bandwidth, were calculated from the coupled-mode equations [8]. Because the depths of the grating-engraved waveguides vary with the thickness of positive photoresist (Ultra-123) filled in the waveguide grooves, the effects of depth variation on the transmission characteristics were analyzed as well in this work. In order to prevent co-directional evanescent coupling for obtaining excellent crosstalk performance, we used highly asymmetric waveguides for the coupler to have compound modes confined to each single waveguide. For the ease of comparison, the cross-sectional dimensions of the narrow waveguides are fixed to 7 μm in width, and 6 μm in depth; the widths of the wide waveguides are fixed to 10 μm as well. The depths, denoted by *d*, of the wide waveguides and the separation gaps, denoted by *s*, of the two waveguides are ranged from 3 to 6 μm, and 2-3 μm,

#143147 - $15.00 USD Received 23 Feb 2011; revised 28 Apr 2011; accepted 1 May 2011; published 18 May 2011

respectively. Figures 8(a) and (b) show the fundamental modes of the single waveguides, and Figs. 8(c) and (d) show the compound modes of the ABC coupler with the condition of $d$ = 4.5 μm, and $s$ = 2 μm. The overlap integrals between the single and compound modes are 91.28% and 91.04% for the first and second modes, respectively. It is noted that the overlap integral between the single and compound modes has a minimum as the depths of the grating-engraved waveguides reduced by 25% from the original depth, i.e. 6 μm (see Fig. 9). The result implies that a maximum transmission loss, caused by co-directional cross power transfer, occurs at a depth difference of 1/4 original depth between two waveguides. Nevertheless, as stated above, the configuration in our case possesses highly asymmetric property. The effective indices of the individual waveguides in the case of Fig. 8 are 1.533054 and 1.532288, as obtained from the simulation.

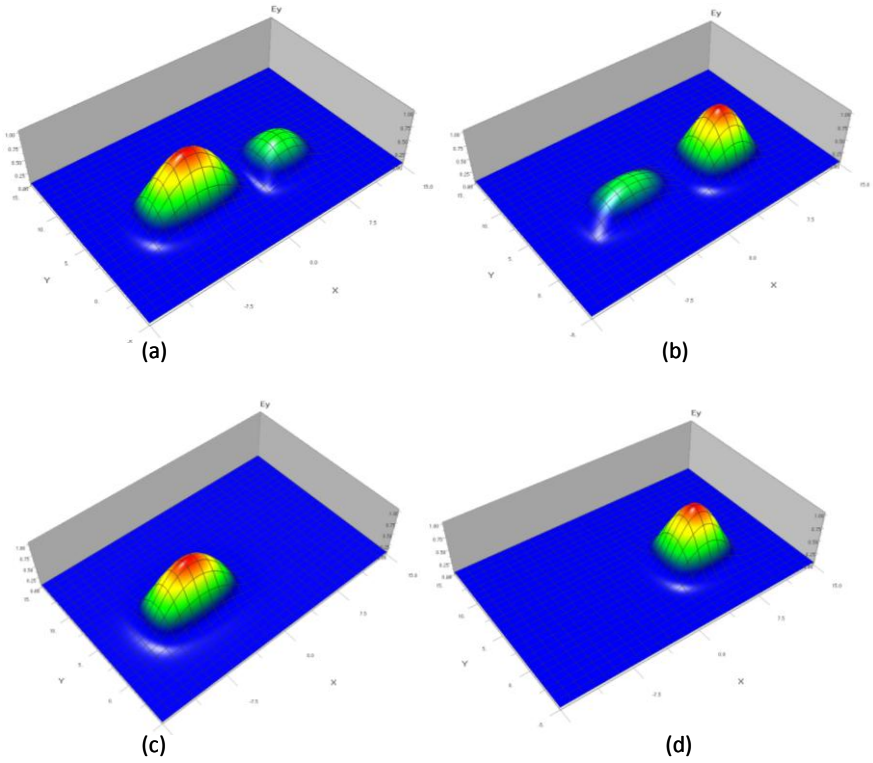


Fig. 8. (a) The first compound mode of the coupler structure; (b) the second compound modes of the coupler (cross-sectional dimension are 4.5 μm × 10 μm and 6 μm × 7 μm gap $s$ = 2 μm; (c) fundamental mode of the single waveguide; width $w$ = 10 μm, depth $d$ = 4.5 μm; (d) fundamental mode of the single waveguide; width $w$ = 7 μm. depth $d$ = 6 μm.

As defined in [8], the coupling coefficient $\kappa_{21}$, concerned with the drop reflectivity and the filtering bandwidth, were calculated from the waveguide mode patterns [8]. Since the co-directional coupling is weak, the minimum transmission, $T_{min}$ in output port can be approximately obtained by $T_{min}$ = 1-$R_{max}$, where $R_{max}$ is the maximum drop reflectivity. It is found the coupling coefficient $\kappa_{21}$ changes with respect to the depths of the grating-engraved waveguides for different separation gaps (see Fig. 9). Here, the grating depth and period were assumed to be 400 nm and 500 nm, respectively. The results show there is a trade-off between the waveguide asymmetry and the coupling coefficient $\kappa_{21}$. The output transmission spectrum of a device with the condition of $d$ = 4.5 μm, $s$ = 2 μm, and coupling length $L$ = 15 mm, was depicted in Fig. 13.

#143147 - $15.00 USD Received 23 Feb 2011; revised 28 Apr 2011; accepted 1 May 2011; published 18 May 2011

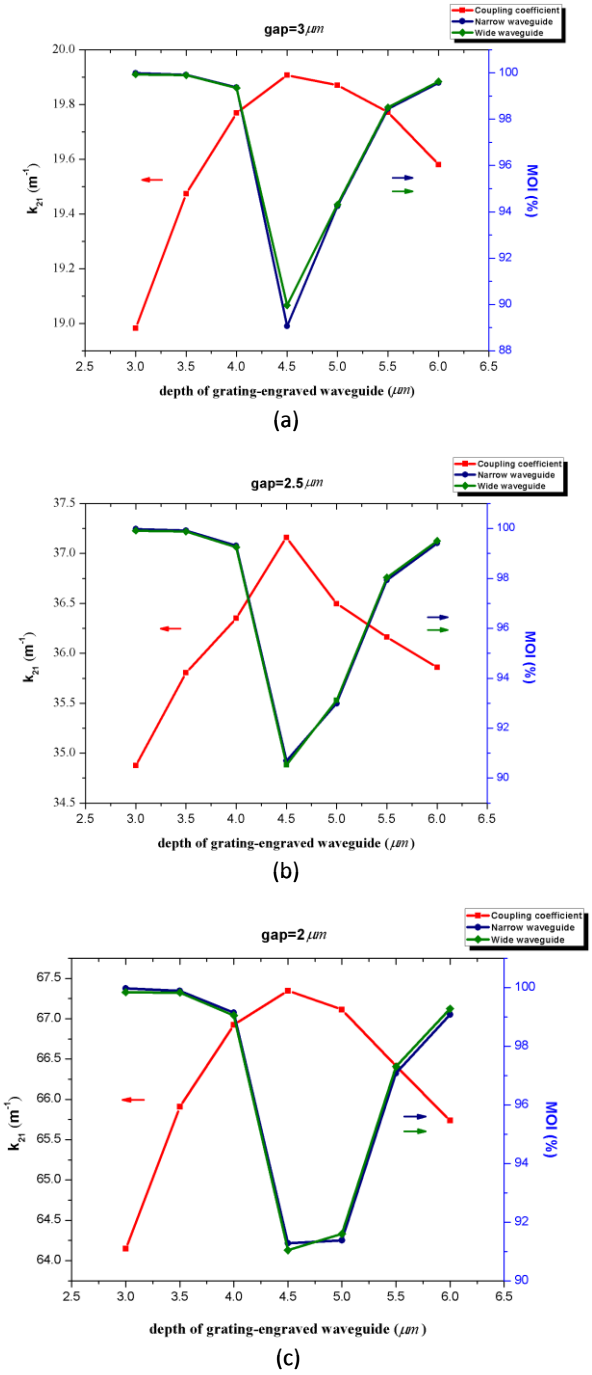


Fig. 9. The coupling coefficient and the compound-individual mode overlap integrals vs. depth of grating-engraved waveguide (a) $s$ = 3 μm; (b) $s$ = 2.5 μm; (c) $s$ = 2 μm. The waveguide widths are 10 μm for wide waveguide and 7 μm for narrow one.

## 4. Measurement

The near-field patterns of the optical waveguides were observed using the end-fire coupling technique. The measurement system was schematically diagramed in Fig. 10. The sample was

#143147 - $15.00 USD Received 23 Feb 2011; revised 28 Apr 2011; accepted 1 May 2011; published 18 May 2011

fixed atop an x-y-z micropositioner (Newport Inc., USA). A single mode optical fiber and microscope objective, used for input light coupling and output image magnification, were also mounted on micropositioners to facilitate the critical alignment. An amplified spontaneous emission (ASE) source, emitting a wavelength range of 1530-1560 nm, was used as the wideband light source (Stabilized Light Source, PTS-BBS, Newport Inc., USA). The light source was polarized in the TE direction, using the in-line polarizer (ILP-55-N, Advanced Fiber Resources, China), which was followed by a polarization controller with an operation wavelength of around 1550 nm (F-POL-PC, Newport Inc., USA). The polarization state was examined by using near infrared precision linear polarizer (20LP-NIR, Newport Inc., USA). The output mode field of the waveguide was imaged onto an IR-CCD (Model 7290, Micron Viewer, Electrophysics Inc., USA) with image analysis software (LBA-710PC-D, V4.17, Spiricon Inc., USA) to show the single-mode characteristics of the waveguide. Figure 11 shows the field intensity distribution of the two output waveguides for the device (the cross sectional dimension are 4.5 μm × 10 μm and 6 μm × 7 μm, and gap $s$ = 2 μm); the ASE laser with power of 3 mW was shone onto the narrow waveguide end (without any gratings) to prevent self-reflection; the asymmetric mode profile was observed as well.

In addition, the insertion, cross-talk, and polarization dependent loss were measured using the same system except that the IR-CCD was replaced by an IR power meter (918D-Ir-OD3 & Model 1918-C, Newport Inc., USA). The utilization of the wideband light source is to avoid optical interference problem. The insertion loss of about 2.5 dB and the cross-talk of about −12.8 dB were obtained for TE polarized light. The polarization dependent loss (PDL) was measured by polarization-scanning method [22] and the result shows that the PDL is about 0.15 dB.

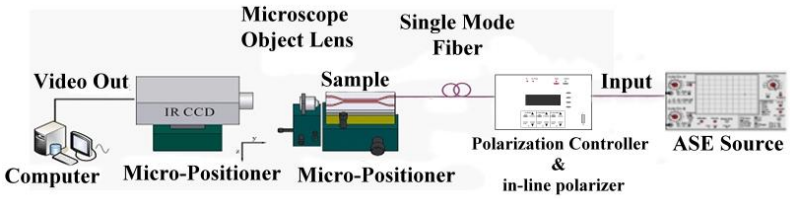


Fig. 10. Schematic of experimental setup for waveguide output mode field measurement.

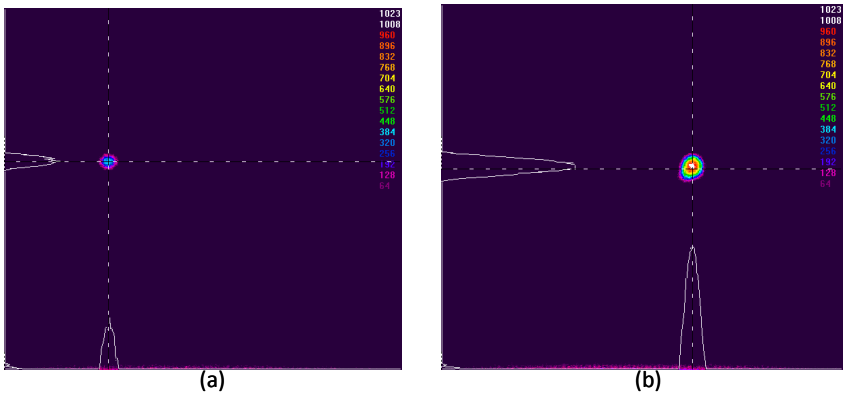


Fig. 11. Near field intensity distribution of two output waveguides: (a) the wide waveguide (with grating), (b) the narrow waveguide (without grating). The ASE laser with the power of 3 mW was shone onto the narrow waveguide.

The spectral characteristics of the non-self-reflection ABC-based filter were measured using a tunable laser system (Agilent 81640A, Agilent Inc., USA). The tunable laser is of a wavelength range of 1511-1562 nm and followed by a polarization controller. The output

#143147 - $15.00 USD Received 23 Feb 2011; revised 28 Apr 2011; accepted 1 May 2011; published 18 May 2011

fiber of the tunable laser is of Panda-type polarization maintaining fiber, with TE mode in the slow axis in line with vertical direction. An alignment He-Ne laser, used as the auxiliary source, was combined with the wideband source using a 2 × 1 optical coupler. The optical filter was fixed atop a micropositioner; two single-mode fibers, used for input and output beam coupling, were also mounted on micropositioners. The input light source was polarized in the TE direction, as was the mode field measurement system. The output fiber was then connected to the receiver end of the tunable laser to characterize the filter performance.

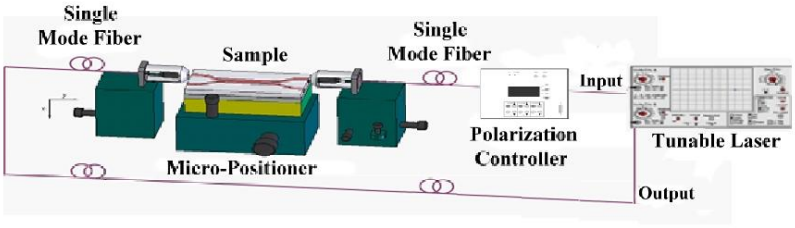


Fig. 12. Schematic of experimental setup for transmission spectrum measurement.

A schematic diagram of the measurement was depicted in Fig. 12. To avoid undesired reflection for optimum device operation, the tunable laser was coupled onto the narrow waveguide ends of the filters and coupled out from the alternative ends of the same waveguides. The measured result which is similar to the theoretical prediction is depicted in Fig. 13. At the Bragg wavelength, a single transmission dip of −9.2 dB was obtained. The measured Bragg wavelength is about 1532.8 nm, which is off approximately 0.13 nm from the theoretical prediction (1532.67 nm). The 3 dB bandwidth of the filter measured is about 0.125 nm, different from the simulation one by 0.025 nm (the theoretical bandwidth is about 0.1 nm). Furthermore, there is a side lobe observed in experiment data at around 1531.6 nm, which might be caused from the Fabry-Perot etalon formed by the plane parallel faces of the fibers and waveguide [23]. We also measured the filter response for TM polarization, which appears similar and almost overlaps with the TE polarization spectrum except for the transmission dip of −9.3 dB. According to the numerical simulation, the central wavelength is expected to be 1532.62 nm, which is shifted off the TE transmission dip merely by 0.05 nm, approaching the resolution of the tunable laser system.

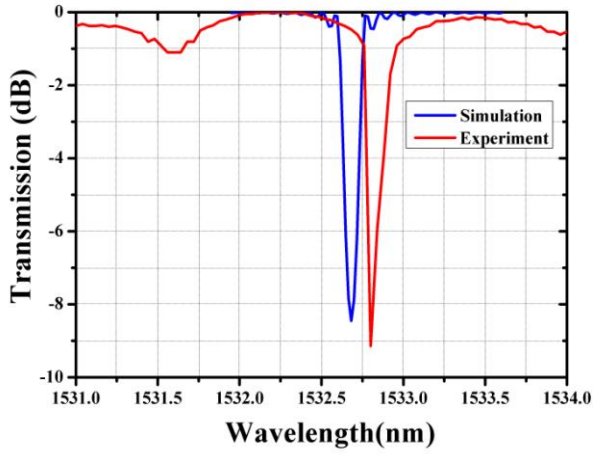


Fig. 13. Transmission spectra of an ABC-based polymeric waveguide filter. The red line represents the experimental result and the blue line represents the simulation result.

#143147 - $15.00 USD Received 23 Feb 2011; revised 28 Apr 2011; accepted 1 May 2011; published 18 May 2011

## 5. Conclusion

We successfully developed a process to fabricate a polymeric waveguide filter based on an asymmetric Bragg coupler with a single-grating waveguide. In this work, a master mold of an asymmetric waveguide coupler was formed first on a negative photoresist, followed by injecting an h-PDMS into the narrow waveguide of the coupler to act as a protection layer; then, a grating pattern was exposed on the alternative waveguide and subsequently transferred to a PDMS mold; following this step, the PDMS mold was used as a stamp to transfer the ABC-based filter onto a UV cure epoxy to form the final filter. Simulation and experiment results demonstrate that the proposed fabrication process is reliable and accurate, which may offer great potential for mass production of any grating structure on either waveguide of polymeric waveguide couplers.

#143147 - $15.00 USD Received 23 Feb 2011; revised 28 Apr 2011; accepted 1 May 2011; published 18 May 2011